Magnetic hardening and spin-glass phenomena in nanocrystalline FeNbB at low temperatures

I. Škorvánek*
Institute of Experimental Physics, Slovak Academy of Sciences, SK-043 53 Košice, Slovakia

S. Skwirblies and J. Kötzler
Institute of Applied Physics, University Hamburg, D-20355 Hamburg, Germany
(Received 16 May 2001; published 24 October 2001)

The soft nanocrystalline alloy $Fe_{80.5}Nb_7B_{12.5}$, containing 25 vol % of bcc Fe, displays a rapid magnetic hardening below 20 K. This interesting process is accompanied by a strong irreversibility between field- and zero-field-cooled magnetizations and by a maximum of the magnetic viscosity near 8 K, both determined in a field of 1 Oe. We investigated the magnetization dynamics in more detail by measuring the linear ac susceptibility $\chi' + i\chi''$ between 30 mHz and 100 kHz. The shifts of the χ'' maxima towards low temperatures with decreasing frequency reveal a critical slowing down of the characteristic time, characterized by a critical exponent $z\nu = 6.9(2)$, and a collective freezing temperature of $T_g = 7.5$ K. The collective nature of the freezing is supported by a dynamical scaling analysis of $\chi''(T,\omega)$, yielding for the order parameter exponent $\beta = 0.40(5)$, in good agreement with results for the spin glasses. We discuss these results by assuming a frustration of the exchange in the disordered interfacial regions and by the presence of the weak magnetic Nb-rich shells around the nanocrystalline grains.

DOI: 10.1103/PhysRevB.64.184437 PACS number(s): 75.50.Tt, 75.50.Lk, 75.60.Ej

I. INTRODUCTION

Nanocrystalline magnetic materials often reveal unique magnetic properties that strikingly differ from their bulk polycrystalline counterparts. Thus, on many occasions, they have proved to be promising candidates for a variety of magnetic applications. Examples include the soft and hard magnetic materials as well as the materials for magnetic recording.[1] Besides their technological relevance, the nanocrystalline materials also represent attractive objects for the fundamental magnetic studies. The magnetic behavior of these systems can vary widely depending on the size of the nanocrystalline particles as well as on the volume fraction and on the magnetic properties of an intergranular matrix phase.

Iron-rich soft magnetic nanocrystalline materials prepared by controlled crystallization of melt-spun amorphous precursors, typically FeCuNbSiB (Ref. 2) and Fe(Zr, Nb)BCu,[3] represent two-phase magnetic systems, where the bcc Fe(Si) or bcc Fe nanocrystalline particles with an average grain size of 10–20 nm are embedded in a residual amorphous matrix. The explanation of the magnetic softness observed in these systems has been given by Herzer[4] based on the random anisotropy model (RAM), which was originally developed for amorphous alloys.[5] He showed that in a single-phase nanocrystalline ferromagnetic system with the random distribution of crystallite orientations the magnetic behavior is determined by the ratio of the particle size D to the exchange correlation length $L_{ex} = \sqrt{A/K}$, where A is the exchange stiffness constant and K is the magnetocrystalline anisotropy constant. The main conclusion of this RAM model is that if D is smaller than the exchange length L_{ex}, then the magnetic moments experience an effective anisotropy $K_{eff} = K/\sqrt{N_c}$, which is strongly reduced due to its averaging over several grains. Here $N_c = (L_{ex}/D)^3$ is the number of crystallites in an exchange coupled volume L_{ex}^3. By eliminating the exchange length between the above expressions, Herzer found that the exchange-averaged anisotropy scales as $K_{eff} = K^4 D^6/A^3$. The value of L_{ex} is typically of tens of nanometers for these systems, and consequently for the smaller grain sizes, the sixth power law represents a very rapid variation of K_{eff} with D. The coercivity is expected to scale with K_{eff}, and hence, the excellent soft magnetic properties are usually observed for $D < 20$ nm.

As the exchange coupling is mediated by the residual matrix phase, its magnetic state plays a very important role in determining the magnetic softness. In order to take better into account the exchange interactions acting over the crystalline-amorphous-crystalline coupling chains, the original single-phase RAM model has been extended to two-phase RAM models, where the relevant magnetic and structural parameters such as the exchange stiffness and the anisotropy constants as well as the volumetric fractions are considered for both the crystalline phase and the amorphous matrix.[6–8] These models allowed to explain two experimentally observed features:

(i) the magnetic hardening at the first stages of nanocrystallization, when the nanocrystals are separated by relatively thick amorphous matrix,

(ii) the magnetic hardening at elevated temperatures, i.e., near the Curie temperature of the residual amorphous phase, $T_c(\mathrm{am})$.

Contrary to the numerous works on Fe-based nanocrystalline alloys at high temperatures, less attention has been devoted to the behavior of the soft magnetic characteristics in these materials at low temperatures. In particular, for temperatures far below the $T_c(\mathrm{am})$, where the nanograins are supposed to be well coupled, the above quoted two-phase RAM models do not predict any drastic changes of the coercive field and, indeed, the existing data for the FeCuNbSiB-type alloys showed only minor changes of coercive field down to helium temperature.[9,10] On the other

hand, some magnetic hardening at low temperatures has been reported by Arcas *et al.*[11] for the melt-spun FeZrBCu alloys containing less than 5×10^{-3} volume fraction of nanocrystalline particles. However, these extremely diluted systems can not be considered as conventional nanocrystalline materials but are rather amorphous with a very small amount of crystalline inclusions. An advanced nanocrystalline sample of FeZrBCu containing a large crystalline fraction of 0.54 exhibited only very shallow decrease of coercive field towards the low temperatures.

On the other hand, in nanocrystalline $Fe_{80.5}Nb_7B_{12.5}$ (Ref. 12) and $Fe_{73.5}Nb_{4.5}Cr_5B_{16}Cu_1$ (Ref. 13) alloys exhibiting medium degrees of nanocrystallinity, a rapid increase of the coercive field by nearly two orders of magnitude has been found at temperatures below 20 K. This magnetic hardening at low temperatures is a novel feature of soft magnetic nanocrystalline materials. In this paper we present the first detailed study of the magnetization dynamics of the nanocrystalline $Fe_{80.5}Nb_7B_{12.5}$ at low temperatures. The experimental background is given in Sec. II. In Sec. III, we characterize the magnetic hardening by measurements of the coercive field and by investigations of the magnetic irreversibilities at low fields. Moreover, we present here the results of magnetization creep at low temperatures. In Sec. IV, the relaxation behavior is determined from the frequency variation of the linear ac susceptibility. The data, in particular the scaling property of the ac absorption, suggest the onset of a collective spin-freezing below 10 K. Possible sources for this collective phenomenon related to the microstructure of the present material are discussed in Sec. V. The main conclusions of our experimental study are given in Sec. VI.

II. EXPERIMENT

Amorphous ribbons of $Fe_{80.5}Nb_7B_{12.5}$ alloy 10 mm wide and 28 μm thick have been prepared by a planar flow casting method from the melt in the Institute of Physics SAS, Bratislava. Pieces of these ribbons were annealed under protective argon atmosphere for 1 h at 510 °C, which provided nanocrystalline samples exhibiting the strongest magnetic hardening at low temperatures. The crystallization behavior was determined by differential scanning calorimetry (DSC),[14] and the structural changes upon annealing were examined by using x-ray diffraction (XRD), transmission electron microscopy (TEM), Mössbauer spectroscopy (MS), and small angle neutron scattering (SANS).[15,16] These investigations have revealed the presence of bcc-Fe nanocrystalline grains with an average diameter of $D=13$ nm embedded in the remaining Nb- and B-enriched amorphous matrix. The volume fraction of the nanocrystalline phase of the sample investigated here was estimated to be $\nu_{cr}=0.26$. Using these results and the relation $d=D(C\nu_{cr}^{-1/3}-1)$, where C ranges from 0.9 to 1 depending on the arrangement,[17] we find for the mean distance between nanocrystalline grains $d\approx0.5D$.

The measurements of the dc magnetization as a function of temperature and applied field have been performed by a commercial superconducting quantum interference device (SQUID) magnetometer (Quantum Design MPMS2) in the range 1.8–300 K. In addition, the magnetization creep after application of small external field of 1 Oe has been investigated at selected temperatures within the magnetic hardening regime. By directly recording the feedback voltage of the SQUID using the optional software of the MPMS2 magnetometer and keeping the sample fixed in the pickup system, it is possible to extend the time window for $M(t)$ down to 0.1 s. The ac susceptibility measurements were also performed by the SQUID, covering frequencies from 30 mHz to 1 kHz at an amplitude of 0.01 Oe, where the response proved to be linear down to lowest temperatures. An extension up to 100 kHz was made by conventional lock-in detection.

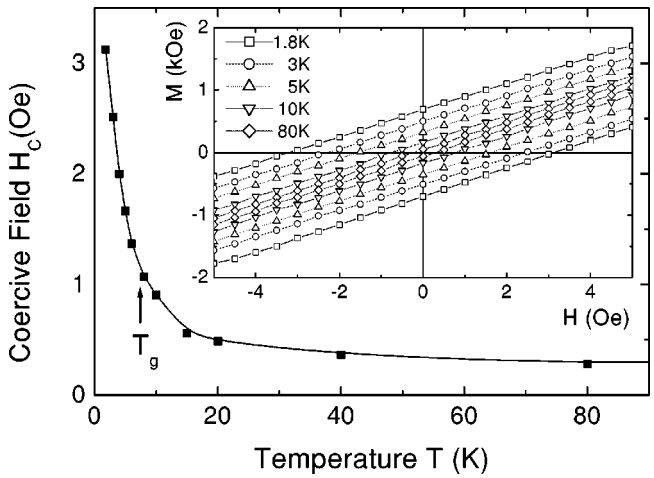

FIG. 1. Temperature variation of the coercive fields, $H_c(T)$, for nanocrystalline $Fe_{80.5}Nb_7B_{12.5}$ annealed at 510 °C for 1 h. Inset shows the low-field portion of hysteresis loops recorded at the indicated temperatures.

III. MAGNETIC IRREVERSIBILITY AND CREEP

In Fig. 1, the magnetic hardening at low temperatures is evidenced by the increase of coercive field H_c. These values were determined from the magnetic hysteresis loops measured by the SQUID magnetometer, the low-field parts of which are shown by the inset of Fig. 1. Upon lowering the temperature from 80 to 1.8 K, the coercive field increases from 0.28 to 3.12 Oe and the major part of this increase takes place at temperatures below 15 K. The irreversibility occurring at low temperature is also reflected by field-cooled (FC), zero-field-cooled (ZFC), and thermoremanent (TMR) magnetization. The sequence of measurements shown in Fig. 2 was as follows: The FC curve was recorded during the cooling from 200 K down to 2 K in an external field of 1 Oe. After reaching 2 K, the field was switched off and the TMR curve was measured during the warming to 200 K. Finally, the sample was cooled again to 2 K at zero field, and after application of 1 Oe the ZFC magnetization was determined during warming to 200 K.

Obviously, in the whole temperature range the FC magnetization remains constant at its maximum value $H/N=200$, which is determined by the demagnetization factor of the sample, N. This implies that the internal susceptibility of the material is much larger than $1/N$ expected for a very soft

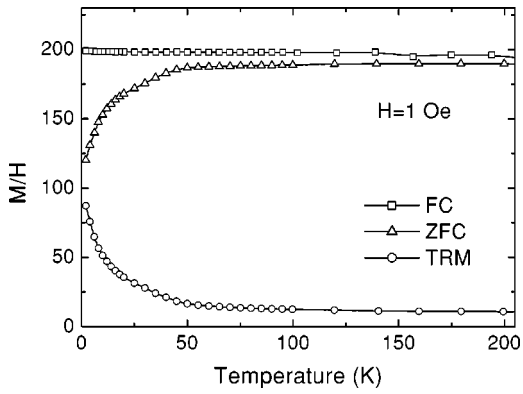

FIG. 2. Field-cooled (FC), zero-field-cooled (ZFC) and thermoremanent (TRM) magnetization as a function of temperature for nanocrystalline $Fe_{80.5}Nb_7B_{12.5}$.

bulk ferromagnet, which in the case of the present materials results from the strong exchange coupling between the nanocrystalline grains mediated by the amorphous matrix. We note that in our case the field was applied parallel to the longest axis of the ribbon sample. Below 50 K, both the ZFC and TMR magnetizations signalize a rather strong magnetic irreversibility, which goes along with the increase of coercive field. It is interesting to note that the sum of M_{ZFC} and M_{TMR} is equal to the equilibrium magnetization $M_{\mathrm{FC}}=H/N$, i.e., they obey the magnetization sum rule, $M_{\mathrm{ZFC}}+M_{\mathrm{TMR}}=H/N$. This indicates that both of the nonequilibrium magnetizations $M_{\mathrm{FC}}-M_{\mathrm{ZFC}}$ and M_{TMR} created at 2 K have the same, rather large values close to $0.4H/N$ and that during the warming they decay on the same time scale. For both quantities we chose the same time of about 80 min to warm the sample from 2 to 50 K.

Similar irreversibility effects have been reported recently for FeZrBCu nanocrystalline alloys at early stages of crystallization.[17] However, the observed effects were much less intense as compared to our system. Furthermore, the authors did not investigate the changes of coercive field with temperature.

In order to provide additional information on the irreversibility, we have also studied the relaxation behavior at fixed temperatures. To this end, the sample was cooled in zero field from 200 K to the temperature of measurement, where the magnetic field of 1 Oe was applied and the time variation of magnetization was recorded up to 100 s. The results for $M(t)$ are depicted in Fig. 3 on a logarithmic scale, the slope of which defines the mean magnetic viscosity $S(T)$. As can be seen in the inset of Fig. 3, $S(T)$ displays a clear maximum near 8 K. Similar peaks in the magnetic viscosity coefficient have also been observed in other inhomogeneous magnetic alloys such as AuFe spin glasses,[18] dipolarly interacting frozen ferrofluids,[19] and giant magnetoresistive CuCo alloys showing spin-glass-like ordering.[20] The close correlation between the peak temperature of S and the upturn of coercive field in our system suggests that that the spin freezing and the magnetic hardening at low temperatures have a common origin. In order to illuminate this correlation further, we investigate now the linear ac susceptibility at zero external field.

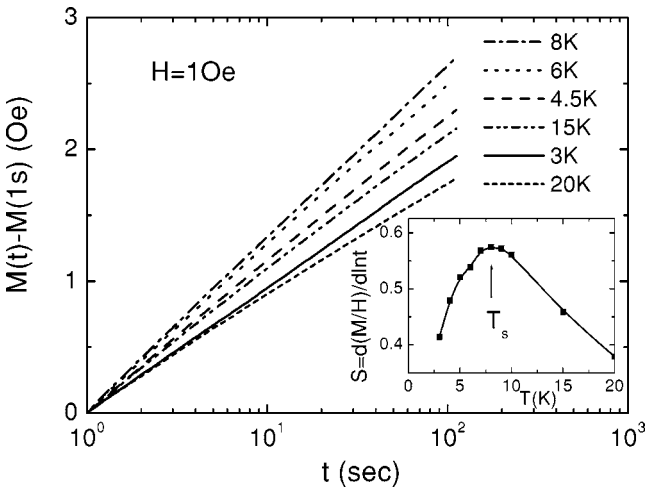

FIG. 3. Time dependencies of the magnetization, $M(t)$, in 1 Oe applied after zero-field cooling to different temperatures. Inset: The temperature variation of mean magnetic viscosity coefficient, $S(T)$.

IV. REVERSIBLE MAGNETIZATION DYNAMICS

The temperature dependencies of the real and imaginary components of the ac susceptibility $\chi(\omega,T)$ measured at different frequencies are shown in Fig. 4. The real (in-phase) component χ' becomes frequency dependent near $T=60$ K, which marked also the onset of the irreversibility in the low field magnetizations (see Fig. 2). This frequency variation of χ' is accompanied by the appearance of a finite imaginary (out-of-phase) χ'', indicating the presence of a relaxation process. Upon increasing ω the maximum of χ'' shifts to a higher temperature, and we may associate with the peak temperature T_ω a mean relaxation time $\tau(T_\omega)=\omega^{-1}$. The results are indicated on an Arrhenius plot shown in Fig. 5, which reveals thermally activated behavior at elevated temperatures, $\tau(T)=\tau_0\exp(E_a/k_BT)$. In this temperature regime we obtain for the activation energy $E_a/k_B=218$ K and for the microscopic relaxation time $\tau_0=5.3\times10^{-12}$ s.

At lower temperatures, the relaxation rates decrease stronger than the Arrhenius law indicating the crossover to a collective magnetic freezing. In this case, we rather expect a power law[21] for the critical slowing down of τ,

$$\tau(T)=\tau_0\left(\frac{T}{T_g}-1\right)^{-z\nu}. \tag{4.1}$$

According to the inset of Fig. 5, we find for the collective freezing temperature of the disordered spin-system $T_g=7.5(2)$ K and for the dynamical exponent $z\nu=6.9(2)$. A value of $\tau_0=1.1\times10^{-5}$ s was obtained for the characteristic flipping time of the magnetic moments.

Figure 5 clearly demonstrates the validity of the power law (4.1) in the whole temperature range under investigation. The value of the critical exponent $z\nu$ is in good agreement with the values obtained for spin-glasses[21] but somewhat smaller than $z\nu=10.5$ reported recently for Fe-C nanoparticles.[22] In this picture of a collective freezing, the rather large τ_0 value may point to a cluster-glass nature of our material. The large magnetic moments of the

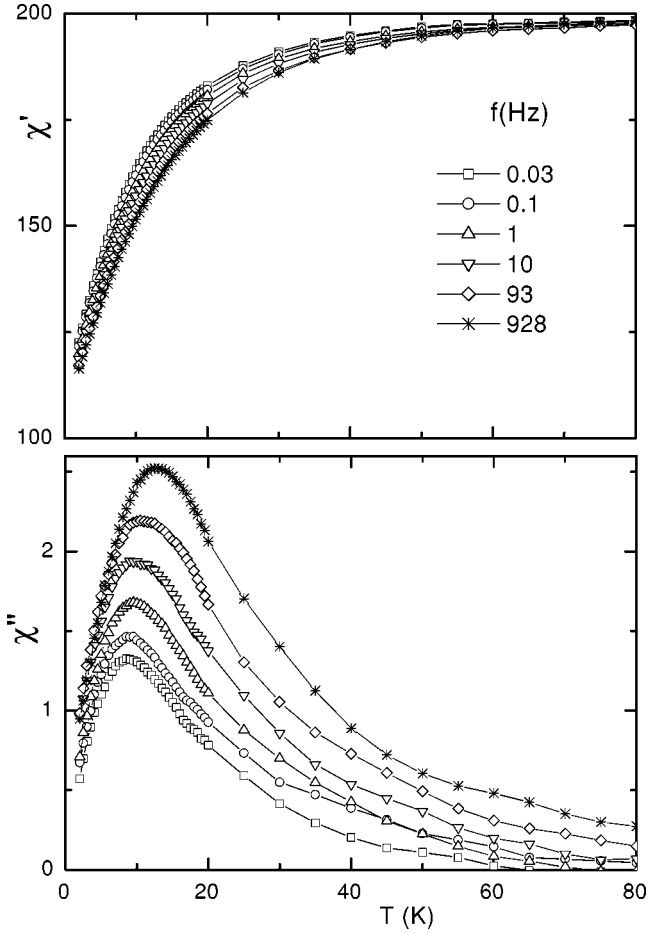

FIG. 4. Temperature dependencies of the dispersion $\chi'(\omega,T)$ and absorption $\chi''(\omega,T)$ measured at different frequencies for nanocrystalline $Fe_{80.5}Nb_7B_{12.5}$.

cluster-glass involved in ''spin-flip'' process were proposed recently also for some other nanoparticle systems.[20,23]

A relevant test of a collective behavior can be obtained by analyzing the frequency and temperature dependences of the absorption component $\chi''(\omega,T)$ of the linear acsusceptibility. Above the ordering temperature T_g of spin glasses, $\chi''(\omega,T)$ is predicted to obey the following dynamic scaling law:[24–26]

$$\chi''(\omega,T)=\left(\frac{T}{T_g}-1\right)^{\beta}F(\omega\tau). \tag{4.2}$$

Here $F(x)$ denotes a still unknown dynamical scaling function and β the exponent describing the temperature variation of the spin-glass order parameter. In fact, Fig. 6 shows a quite convincing collapse of the magnetic absorption data taken at different frequencies on a single curve. The value of $\beta=0.40(5)$ is close to $\beta=0.5$ reported for standard spin glasses and by Monte Carlo simulations based on the $3D$ $\pm J$ model.[25,26]

V. DISCUSSION

The magnetic hardening at low temperatures in Fe-based nanocrystalline alloys seems to depend sensitively on the metallurgical state of the investigated samples. As it has been pointed out in Sec. I, the abrupt increase of the coercive field at low temperatures was not observed for the most frequently investigated soft magnetic nanocrystalline alloy families such as FeCuNbSiB or FeZrBCu. Moreover, even for the present composition, the strength of the magnetic hardening at low temperatures depends strongly on the volume fraction of nanocrystalline particles.[12] These observations clearly indicate that among the relevant microstructural parameters, which seem to govern this behavior are the nature of intergranular phase that separates nanocrystalline bcc Fe grains and the concentration of the latter. Therefore, in order to discuss the possible sources of the magnetic hardening and the spin-glass-like features in our system, we shall firstly focus our attention to the processes, which control the development of the microstructure during annealing of this particular composition.

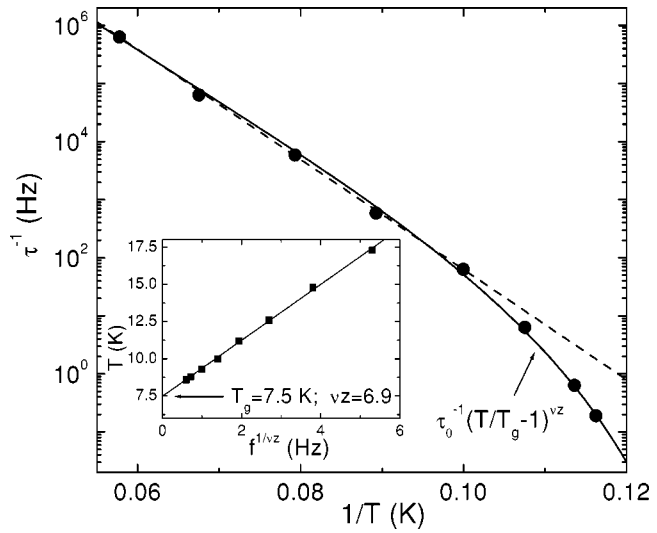

FIG. 5. The shift of the χ'' maxima fitted by both the Arrhenius law for thermal activation (dashed line) and by the power law Eq. (4.1). The straight line in the inset defines the value of the critical exponent $z\nu$ and the freezing temperature T_g.

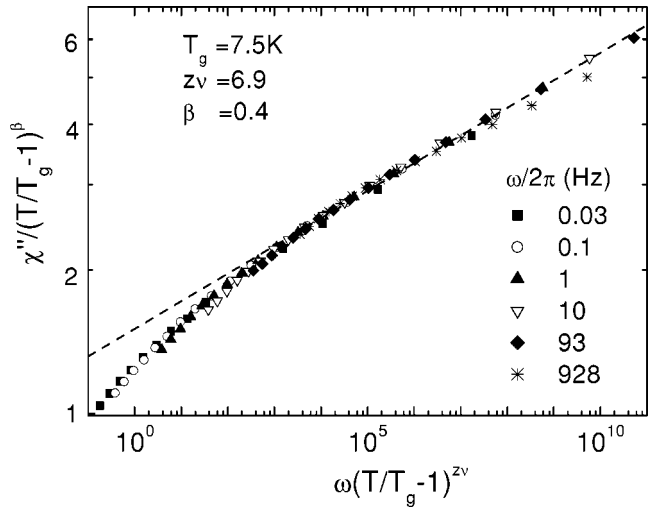

FIG. 6. Dynamical scaling analysis of $\chi''(\omega,T)$ data for $T>T_g$ according to Eq. (4.2). Symbols refer to different frequencies.

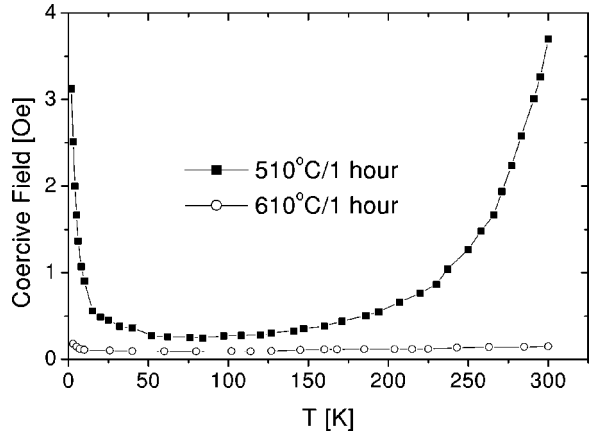

FIG. 7. Temperature dependencies of the coercive field, $H_c(T)$, for the $Fe_{80.5}Nb_7B_{12.5}$ samples containing different volume fraction of nanocrystalline particles.

The amorphous $Fe_{80.5}Nb_7B_{12.5}$ alloy clearly shows a two-stage nature of the primary crystallization process.[14] The first and second stage of this process have been described by the nucleation and growth and by grain-growth mechanisms, respectively.[27] Obviously, it is the niobium content that plays a decisive role in controlling the crystallite size in FeNbB alloys. This element acts as a slowly diffusing inhibitor accumulating in front of the growing interface of the bcc Fe grains leading to a diffusion barrier that finally stops the growth process. A direct microstructural evidence of such an accumulation of slowly diffusing atoms in the close vicinity of nanocrystalline Fe grains in amorphous matrix has been provided by using the atom probe field ion microscopy technique.[28] The increasing Nb content is known to suppress significantly the Curie temperature as well as the saturation magnetization value in FeNbB alloys.[29] Hence, the presence of the Nb-enriched shells in the nearest vicinity of grains should be reflected by magnetically weaker regions at the interphases between the bcc Fe crystallites and the residual matrix, leading to a reduced magnetic coupling between grains. For the present sample exhibiting a medium degree of crystallinity, it seems that the concentration gradient of Nb at the interface between the nanocrystals and the remaining amorphous matrix could be particularly significant.[14] A presence of the weak magnetic Nb-rich shells created around the crystallites for this sample is indicated also by the Mössbauer spectrometry, revealing a remarkable population of the low hyperfine fields in the hyperfine field distribution of the intergranular amorphous phase even at cryogenic temperatures.[16] On the other hand, in accordance with a two-stage nature of the crystallization process, a concentration gradient of Nb at the crystalline/amorphous interface can be reduced by an increased diffusion of Nb at higher annealing temperatures leading to its more homogeneous spreading over the remaining amorphous matrix, thus allowing the grains to grow further. Figure 7 shows that after annealing for 1 h at 610 °C, which leads to the advanced stage of nanocrystallization containing a crystalline fraction of 0.62, both the low- and the high-temperature magnetic hardenings are significantly reduced as compared to the sample annealed at 510 °C investigated in our study.

We shall now focus our attention on the microstructural factors, which could affect the freezing of the magnetic moments in our system. Spin-glass features in the low temperature magnetic behavior of different nanosized systems such as ball-milled pure nanocrystalline iron,[30] ferromagnetic $NiFe_2O_4$ nanoparticles,[31] FeZrB nanocrystalline alloys,[32] or ball-milled Fe-Rh powders[33] have been assigned to some spin disorder located at the structurally disordered interfaces and/or outer shells of the magnetic nanoparticles. We assume that this may be also the case of the present sample. Here the highly disordered regions may be associated with the interfaces between nanocrystalline grains and the amorphous matrix. The accumulation of larger Nb atoms near such interfaces and the related stress fields could even enhance a degree of structural disorder. Due to the variations of the Fe-Fe nearest-neighbor interatomic spacings within these topologically disordered regions, which include or which may be in close contact with the spins of the surface layers of the nanocrystalline grains, the exchange interactions can vary by magnitude and even by sign. As a consequence of competing exchange interactions, severe frustrations may produce spin-glass behavior of the interfacial regions.

In order to discuss the observed magnetic hardening at low temperatures within the context of the RAM, we should also consider in addition to the crystalline phase and the amorphous matrix phase the presence of the grain/matrix interfacial regions. At low temperatures, the relevant material parameters of the crystalline and the amorphous residual phase such as the magnetic anisotropy constant and the exchange constant depend rather weakly on the measuring temperature. Therefore, one would not expect any drastic changes of coercive field at low temperature. However, a different situation may exist for the interfacial regions. Here, the onset of magnetic frustration may result in an increase of local anisotropy if the spins at the grain/matrix interfaces are frozen in random directions. By analogy to similar considerations for the spins in the grain boundary layers of pure nanocrystalline iron particles,[30] one may assume that in the interfacial regions the exchange correlation length L_{ex} becomes smaller than the mean thickness of these regions. In such a case, the exchange coupling between the spins belonging to adjacent grains is strongly reduced, so that the anisotropy may become significant in determining the magnetic behavior of the overall system. Consequently, all Fe spins located within the nanocrystalline grains may align with the local randomly oriented easy axes to form a cluster-glass state. This interpretation seems to be in agreement with our results reported in Sec. IV, which indicate the presence of collective magnetic dynamics and critical slowing down approaching the glass temperature T_g from above. The value of T_g coincides well with the temperature below which the most pronounced changes of coercivity take place. In addition the high value of the microscopic relaxation time τ_0 supports a cluster-glass nature of the investigated material.

We emphasize that the important role in the above scenario is played by the weak magnetic Nb-rich shells around the crystallites in our sample. These shells may effectively reduce the strength of exchange coupling between the spins

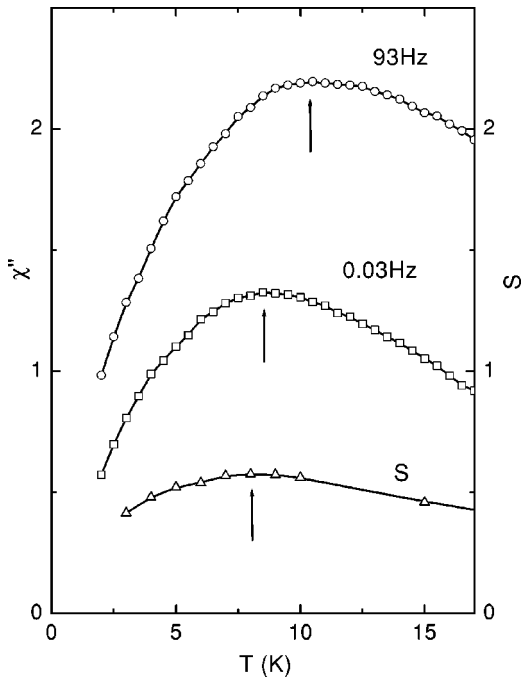

FIG. 8. The temperature variation of the mean magnetic viscosity, $S(T)$, and of the out-of-phase component of the ac susceptibility, $\chi''(\omega,T)$. The shift of the maximum to lower temperatures upon the increase of observation time is indicated by arrows.

located at the surface layers of the nanocrystalline grains on the one side and the spins located in the residual amorphous matrix phase on the other side of these weak magnetic regions. A consequent shielding of the exchange coupling shall facilitate the freezing of spins at the structurally disordered interfaces. On the other hand, for the nanocrystalline samples without the Nb-enriched shells around the crystallites or for significantly smaller intergrain distances, the exchange coupling will be strong enough to prevent them from freezing in random directions. Consequently, the magnetic hardening at low temperatures for samples with higher degree of crystallinity is diminished.

The strong irreversibility between ZFC and FC magnetization curves reported in Sec. III is related to the difference between the random distribution of magnetic moments of the grains and the fully ordered state which can be obtained after cooling the system in an even weak applied field. This indicates that the multiple degenerate spin configurations exist at low temperatures and weak applied fields. In the ZFC regime the magnetization of the frozen state will react in time to any change of external field. The external field has to overcome an array of the random local anisotropy axes before the various clusters can align with the field. Clearly, the increase of temperature will facilitate this process due to the thermally assisted jumps of the cluster moments away from their anisotropy-pinned ''frozen'' orientation.

Our results obtained by different experimental techniques, indicate a significant slowing down of the magnetization dynamics. The close relation between the magnetization creep and ac susceptibility is evident from Fig. 8. For a slow relaxation of the time-dependent magnetization $M(t)$, a relation between the magnetic viscosity S and the out-of-phase component of ac-susceptibility χ'' exists,[34]

$$S(t)=\frac{1}{H}\frac{dM}{d\ln t}\sim\frac{2}{\pi}\chi''(\omega), \tag{5.1}$$

where $t=\omega^{-1}$ denotes the observation time. This combination of the ac susceptibility and the time-dependent magnetization measurements opens a broader window of observation to study the spin-glass relaxation processes. Here the temperature of the maximum of the magnetic viscosity observed at $T_s=8.0(2)$ K fits well on the $\tau(T)$ curves shown in the main panel and the inset of Fig. 5, if $\tau(T_s)=2\pi\times100$ s, corresponding to our mean measuring time of 100 s (see Fig. 3) is used.

VI. CONCLUSIONS

In summary, a strong increase of the coercive field at cryogenic temperatures in the nanocrystalline $Fe_{80.5}Nb_7B_{12.5}$ was found to be closely correlated with the presence of spin-glass-like phenomena in this alloy. The irreversibility between ZFC and FC magnetization curves, which goes along with the increase of coercive field, starts to develop below 50 K. The ZFC and TMR data show that magnetization will react in time to any change of the low external field while in the frozen state. We conjecture that this slow magnetization process is associated with the magnetic moments of the nanocrystalline grains and/or highly distorted interfaces frozen in their random local anisotropy orientations.

The magnetic creep experiments have shown that the magnetization relaxation on the long time scales is logarithmically slow. An analysis of the frequency dependence of the peak temperature T_ω of the χ'' has shown that the magnetization dynamics of the $Fe_{80.5}Nb_7B_{12.5}$ nanocrystalline sample exhibits a spin-glass-like critical slowing down close to the extracted glassy temperature $T_g=7.5$ K. The values of the dynamical critical exponent $z\nu=6.9(2)$ and the exponent $\beta=0.40(5)$ are compatible with those predicted for spin-glass systems. The large microscopic relaxation time $\tau_0=1.1\times10^{-5}$ s accounts for the cluster-glass nature of investigated material.

The results of this study clearly indicate a collective nature of the spin-freezing process. A possible source of this collective phenomenon is the frustration of the exchange in the disordered interfacial regions, which include and/or which are in close contact with the spins of the surface layers of the nanocrystalline grains. The significant role in the spin freezing seems to be played by the presence of the weak magnetic Nb-rich shells around the nanocrystalline grains, which reduce the intensity of the exchange coupling between the nanocrystals and amorphous matrix.

ACKNOWLEDGMENTS

This work was supported by the Volkswagen Foundation under Project No. VW-I/75961. The authors acknowledge Dr. P. Duhaj and Dr. P. Švec for providing the amorphous samples.

*Electronic address: skorvi@saske.sk
[1] R. C. O'Handley, *Modern Magnetic Materials: Principles and Applications* (Wiley, New York, 1999), p. 432.
[2] Y. Yoshizawa, S. Oguma, and K. Yamaguchi, J. Appl. Phys. **64**, 6044 (1988).
[3] K. Suzuki, A. Makino, A. Inoue, and T. Masumoto, J. Appl. Phys. **70**, 6232 (1991).
[4] G. Herzer, IEEE Trans. Magn. **26**, 1397 (1990).
[5] R. Alben, J. J. Becker, and M. C. Chi, J. Appl. Phys. **49**, 1653 (1978).
[6] G. Herzer, Scr. Metall. Mater. **33**, 1741 (1995).
[7] A. Hernando, M. Vasquez, T. Kulik, and C. Prados, Phys. Rev. B **51**, 3581 (1995).
[8] K. Suzuki and J. M. Cadogan, Phys. Rev. B **58**, 2730 (1998).
[9] B. Hofmann, T. Reininger, and H. Kronmüller, Phys. Status Solidi A **134**, 247 (1992).
[10] D. Holzer, I. Perez de Albeniz, and R. Grössinger, J. Magn. Magn. Mater. **203**, 82 (1999).
[11] J. Arcas, A. Hernando, J. M. Barandiarán, C. Prados, M. Vázquez, P. Marín, and A. Neuweiler, Phys. Rev. B **58**, 5193 (1998).
[12] I. Škorvánek, P. Duhaj, and R. Grössinger, J. Magn. Magn. Mater. **215-216**, 431 (2000).
[13] I. Škorvánek, R. Grössinger, J. Magn. Magn. Mater. **226-230**, 1473 (2001).
[14] I. Škorvánek, J. Kováč, J. Marcin, P. Duhaj, and R. Gerling, J. Magn. Magn. Mater. **203**, 431 (1999).
[15] J. Marcin, A. Wiedenmann, I. Škorvánek, Physica B **276–278**, 870 (2000).
[16] I. Škorvánek, J. Kováč, J.-M. Greneche, J. Phys.: Condens. Matter **12**, 9085 (2000).
[17] J. S. Garitaonandia, P. Gorria, L. Fernández Barquín, and J. M. Barandiarán, Phys. Rev. B **61**, 6150 (2000).
[18] C. N. Guy, J. Phys. F **8**, 1309 (1978).
[19] W. Luo, S. R. Nagel, T. F. Rosenbaum, and R. E. Rosensweig, Phys. Rev. Lett. **67**, 2721 (1991).
[20] B. Idzikowski, U. K. Rösler, D. Eckert, K. Nenkov, and K.-H. Müller, Europhys. Lett. **45**, 714 (1999).
[21] K. Binder and A. P. Young, Rev. Mod. Phys. **58**, 801 (1986).
[22] P. Jönsson, M. F. Hansen, P. Svedlindh, and P. Nordblad, J. Magn. Magn. Mater. **226-230**, 1315 (2001).
[23] C. Djuberg, P. Svedlindh, P. Nordblad, M. F. Hansen, F. Bødker, and S. Mørup, Phys. Rev. Lett. **79**, 5154 (1997).
[24] N. Bontemps, J. Ferré, and A. Mauger, J. Phys. Colloq. **8**, 1063 (1988).
[25] P. Nordblad and P. Svendlindh, in *Spin Glasses and Random Fields*, edited by P. A. Young (World Scientific, Singapore, 1997).
[26] J. A. Mydosh, Spin Glasses: *An Experimental Introduction* (Taylor & Francis, London, 1993).
[27] K. Suzuki, J. M. Cadogan, J. B. Dunlop, and V. Sahajwalla, Appl. Phys. Lett. **67**, 1369 (1996).
[28] A. Inoue, A. Takeuchi, A. Makino, and T. Matsumoto, Sci. Rep. Res. Inst. Tohoku Univ. A **42**, 143 (1996); Y. Zhang, K. Hono, A. Inoue, A. Makino, and T. Sakurai, Acta Math. **44**, 1497 (1996).
[29] K. Suzuki, J. M. Cadogan, V. Sahajwalla, A. Inoue, and T. Masumoto, Mater. Sci. Eng., A **226-228**, 554 (1997).
[30] E. Bonetti, L. Del Bianco, D. Fiorani, D. Rinaldi, R. Caciuffo, and A. Hernando, Phys. Rev. Lett. **83**, 2829 (1999).
[31] R. H. Kodama, A. E. Berkowitz, E. J. McNiff, Jr., and S. Foner, Phys. Rev. Lett. **77**, 394 (1996); J. Appl. Phys. **81**, 5552 (1997).
[32] A. Slawska-Waniewska and J. M. Greneche, Phys. Rev. B **56**, R8491 (1997).
[33] A. Hernando, E. Navarro, M. Multigner, R. Yavari, D. Fiorani, M. Rosenberg, G. Filoti, and R. Caciuffo, Phys. Rev. B **58**, 5181 (1998).
[34] L. Lundgren, P. Svedlindh, and O. Beckman, Phys. Rev. B **26**, 3990 (1982).